

**SB-253514 and Analogues: Novel Inhibitors of Lipoprotein Associated Phospholipase A<sub>2</sub>****Produced by *Pseudomonas fluorescens* DSM 11579****II. Physico-chemical Properties and Structure Elucidation**DAVID J. BUSBY<sup>a</sup>, ROYSTON C. B. COPLEY<sup>a</sup>, JUAN A. HUESO<sup>b</sup>,  
SIMON A. READSHAW<sup>\*a</sup> and ALFONSO RIVERA<sup>b</sup><sup>a</sup>SmithKline Beecham Pharmaceuticals,  
New Frontiers Science Park, Third Avenue, Harlow, Essex, CM19 5AW, UK<sup>b</sup>SmithKline Beecham Pharmaceuticals S.A., Centro de Investigación Básica, Parque Tecnológico de Madrid,  
c/Santiago Grisolia, 28760 Tres Cantos, Madrid, Spain

(Received for publication January 11, 2000)

A series of novel inhibitors of lipoprotein associated phospholipase A<sub>2</sub> were isolated from the culture broths of *Pseudomonas fluorescens* strain DSM11579. The inhibitors fall into two structurally isomeric classes each of which comprise compounds incorporating glycosylated hydrocarbon chains. The structure elucidation for the major member of each structural class is reported. The crystal structure of a non-glycosylated analogue of the 5,5-series, produced through biotransformation, is also reported.

Lipoprotein associated phospholipase A<sub>2</sub> (LpPLA<sub>2</sub>) is the enzyme responsible for hydrolysis of modified oxidised phospholipids from modified low density lipoprotein causing the release of pro-inflammatory lyso-phosphatidyl choline and oxidatively modified fatty acids. Inhibition of LpPLA<sub>2</sub> could therefore form a novel therapeutic strategy in the treatment of diseases that have an inflammatory component such as atherosclerosis. In the course of screening to obtain LpPLA<sub>2</sub> inhibitors from micro-organisms, two series of metabolites of *Pseudomonas fluorescens* strain DSM11579 showed potent inhibitory activity. The taxonomy and fermentation of the producing strain, the isolation of novel LpPLA<sub>2</sub> inhibitors and their biological activities are reported in the preceding article<sup>1)</sup>. In this article the physico-chemical properties and structure elucidation of the major metabolite of each class are presented. Biotransformation to produce non-glycosylated analogues<sup>2)</sup> provided a compound that proved suitable for single crystal X-ray studies and the resulting structure is presented.

**Results and Discussion**

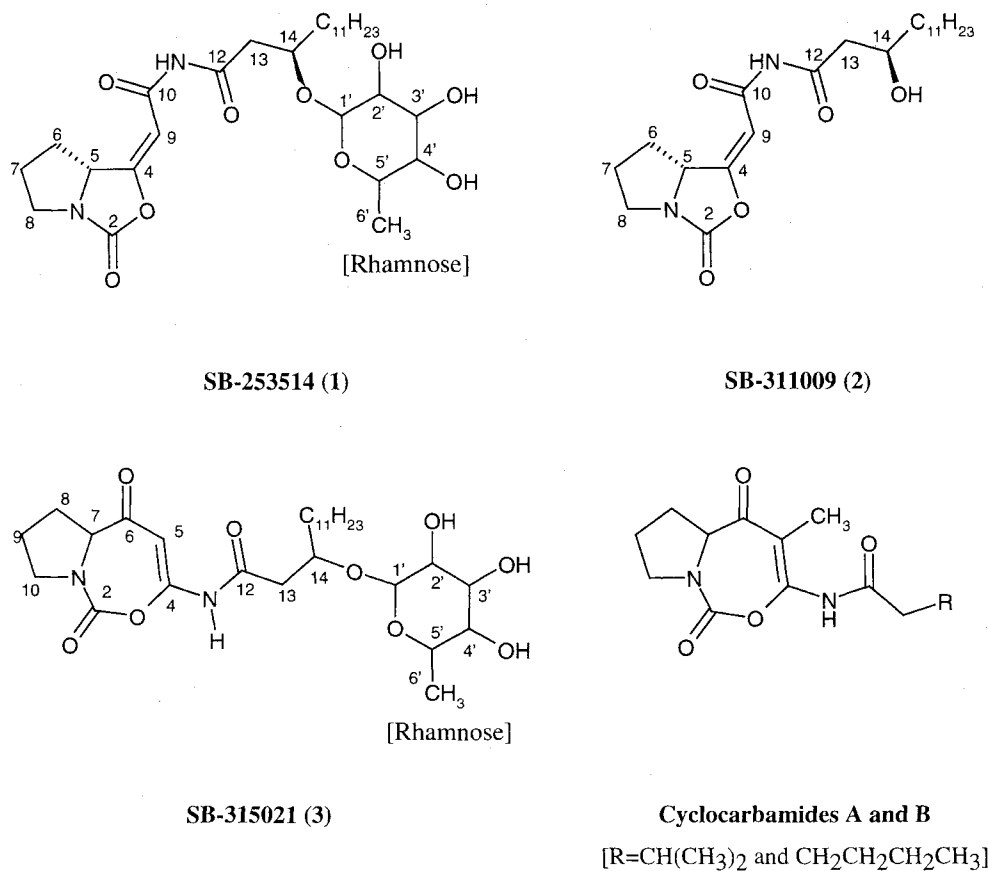
The physico-chemical properties of the metabolites are described in Table 1. The metabolites were all soluble in methanol, ethyl acetate and dichloromethane. Differences in UV maxima (252/251 nm versus 280 nm) were used to identify metabolites from each of the two isomeric classes. The structural significance of the physico-chemical data will be discussed in the following structure elucidations.

**Structure of SB-253514**

SB-253514 represents the major component of the more stable metabolite family. A molecular formula of C<sub>28</sub>H<sub>46</sub>N<sub>2</sub>O<sub>9</sub> was determined for SB-253514 based on the accurate mass measurement and NMR data, which showed the presence of 28 carbons (including two pairs of coincident resonances) and 46 protons (of which 4 were labile). This molecular formula equates to 7 double bond equivalents comprising three carbonyls ( $\delta_C$  at 172.4, 165.9 and 157.0 ppm), one double bond (*sp*<sup>2</sup> carbons at 168.1 and 97.6 ppm) and three rings.

Table 1. Physico-chemical properties.

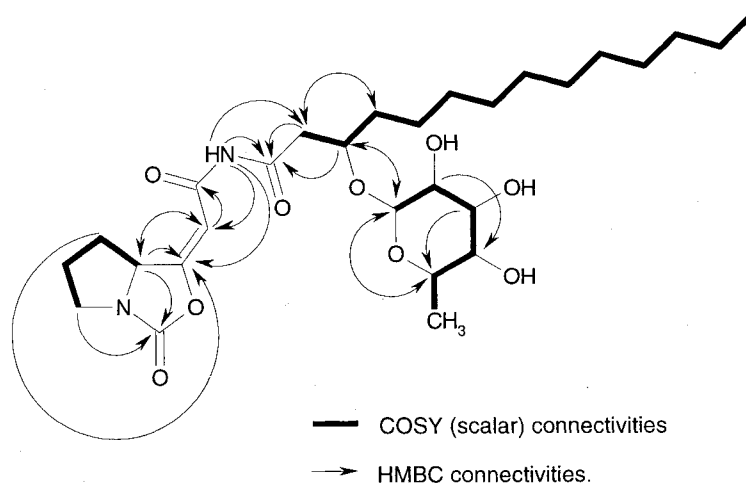
	SB-253514 (1)	SB-311009 (2)	SB-315021 (3)
Appearance	White Powder	White Powder/ Colourless Crystals	Off White Powder
Molecular Formula	C <sub>28</sub> H <sub>46</sub> N <sub>2</sub> O <sub>9</sub>	C <sub>22</sub> H <sub>36</sub> N <sub>2</sub> O <sub>5</sub>	C <sub>28</sub> H <sub>46</sub> N <sub>2</sub> O <sub>9</sub>
HR-FAB MS (MH <sup>+</sup> )	555.3206	409.2686	not determined
HR-ESMS (MH <sup>+</sup> )	555.3272	409.2695	555.3293
calc.	555.3282	409.2702	555.3282
UV λ <sub>max</sub> nm (ε)	252 (14,900 MeOH)	251 (16,300 EtOH)	280 (10,400 EtOH)
IR ν <sub>max</sub> cm <sup>-1</sup>	1804, 1738, 1684, 1651	1792/1778 (split), 1727, 1682, 1639	1738, 1667, 1629

Fig. 1. Structures of the novel LpPLA<sub>2</sub> inhibitors and related cyclocarbamides.

Analysis of the NMR data (aided by 2D COSY connectivities) identified three proton-proton scalar coupled sub-structures resulting from a  $\beta$ -substituted myristyl chain,

a hexose sugar and an *N*-acyl,  $\alpha$ -substituted pyrrolidine (see Figure 2). Identification of the hexose sugar as  $\alpha$ -rhamnopyranose followed from the observed proton-proton

Fig. 2. NMR-derived connectivities for SB-253514 (1).



couplings ( $J_{H1',H2'}=1.6$  Hz,  $J_{H2',H3'}=3.4$  Hz,  $J_{H3',H4'}=9.4$  Hz and  $J_{H4',H5'}=9.4$  Hz) and the hexose  $^{13}\text{C}$  NMR chemical shifts<sup>3</sup>). Long-range, carbon-proton couplings observed in 2D Heteronuclear Multiple Bond Correlation (HMBC) experiments (see Figure 2) confirmed the position of the glycosidic bond and indicated the nature of the atoms connecting the pyrrolidine methine to the myristyl chain. This latter connectivity was also supported by the secondary isotope effects arising from partial deuteration of the labile NH. The position of the "NH" relative to the myristyl chain was confirmed by the 2- and 3-bond isotope shifts observed for carbonyl carbon C12 ( $^2\Delta\delta_{\text{C}}=90$  ppb) and methylene carbon C13 ( $^3\Delta\delta_{\text{C}}=35$  ppb). Isotope shifts of similar magnitude ( $^2\Delta\delta_{\text{C}}=82$  ppb and  $^3\Delta\delta_{\text{C}}=38$  ppb) identified the carbons at 165.9 and 97.6 ppm as C10 and C9, respectively.

Unfortunately the HMBC and secondary isotope data did not provide any information on the cyclisation of the bicyclic system other than positioning a carbamate moiety on the pyrrolidine nitrogen. Cyclisation to yield the 5,5-bicyclic structure (1), as opposed to the 5,7-bicyclic structure (3), followed from a chemical shift analysis and the observation of a 4-bond coupling between the pyrrolidine methine (H5) and the olefinic proton (H9). The chemical shift analysis focused on the carbon adjacent to the pyrrolidine methine which was identified as having a chemical shift of 168.1 ppm. Such a chemical shift would be inconsistent with the  $\alpha,\beta$ -unsaturated ketone carbon (C6) of the 5,7-bicyclic structure (*cf.* cyclocarbamides A and B<sup>4</sup>) but more consistent with the unsaturated C4

carbon of the 5,5-bicyclic structure. Further evidence for the 5,5-structure was provided by the infrared data and in particular the high frequency of the carbamate carbonyl stretching vibration at  $1804\text{ cm}^{-1}$ . Other significant stretching vibrations occur at 1738, 1684 and  $1651\text{ cm}^{-1}$ ; these are consistent with the C12 and C10 carbonyls and the C4-C9 exocyclic double bond, respectively, in the elucidated structure. The exocyclic double bond also gave a characteristically strong band in the Raman spectrum at  $1648\text{ cm}^{-1}$ .

#### Structure of SB-311009

In an attempt to improve the *in vitro* and *in vivo* activity of these metabolites, non-glycosylated analogues were produced *via* biotransformation<sup>2</sup>. The structure of SB-311009, the biotransformation product derived from SB-253514, is presented to support the elucidated structure of the parent metabolite.

Analysis of the NMR data relative to SB-253514 (see Table 2) clearly showed that SB-311009 did not possess the sugar moiety but otherwise was structurally identical. [ $\Delta\delta_{\text{H}}<0.05$  ppm and  $\Delta\delta_{\text{C}}<0.2$  ppm except for H13-H16 and C12-C16]. Furthermore, the non-glycosylated analogue was more crystalline and it was possible to obtain crystals suitable for X-ray diffraction studies by slow evaporation of a methanol solution at  $7^{\circ}\text{C}$ . The crystallographic asymmetric unit contained four independent molecules, subsequently described as molecules A to D (molecules A and B are shown in Figure 3). The absolute configuration

Table 2. NMR assignments in acetone- $d_6$  (chemical shifts in ppm,  $J$  values in Hz).

Atom	SB-253514 (1)		SB-311009 (2)		SB-315021 (3)	
	$\delta_C$	$\delta_H$	$\delta_C$	$\delta_H$	$\delta_C$	$\delta_H$
2	157.0	-	157.0	-	149.6	-
4	168.1	-	168.1	-	154.9	-
5	65.5	4.96 ddd,9.4,6.7,2.0	65.5	4.96 ddd,9.4,6.6,2.0	97.6	6.58 s
6	30.8	2.61 dddd,12.5,6.6,6.6,4.0 1.68 dddd,12.5,9.4,9.4,9.4	30.7	2.61 dddd,12.5,6.5,6.5,4.1 1.67 dddd,12.5,9.4,9.4,9.4	191.1	-
7	26.8	2.12 m	26.8	2.13 m	64.2	4.61 dd,7.9,2.8
8	46.7	3.60 m 3.29 ddd,11.1,8.1,5.3	46.7	3.60 ddd,11.1,7.8,7.8 3.29 ddd,11.1,8.0,5.4	25.3	2.57 m 1.94 m
9	97.6	6.56 d,1.9	97.5	6.58 d,1.9	24.2	1.94 m 1.72 m
10	165.9	-	165.8	-	48.6	3.45 m
11	-	9.66 bs	-	9.71 bs	-	9.50 bs
12	172.4	-	173.2	-	171.0	-
13	43.8	2.89 dd,15.2,7.7 2.79 dd,15.2,5.0	45.9	2.72 dd,15.5,3.9 2.64 dd,15.5,8.2	43.7	2.80 dd,14.3,4.5 2.62 dd,14.3,4.5
14	74.1	4.19 dddd,7.7,5.6,5.6,5.1	68.4	4.05 bm	74.3	4.16 m
15	34.1	1.59 m	38.0	1.49 m	33.9	1.59 m
16	25.5	1.38 m	26.2	1.49 m 1.36 m	25.3	1.36 m
17-22	~30.3	1.29 m	~30.3	1.29 m	~30.3	1.29 m
23	32.6	1.29 m	32.6	1.29 m	32.6	1.29 m
24	23.3	1.29 m	23.3	1.29 m	23.3	1.29 m
25	14.3	0.88 t,6.9	14.3	0.88 t,6.9	14.3	0.88 t,6.7
1'	99.5	4.83 d,1.6	-	-	99.2	4.82 bs
2'	72.3	3.76 bm	-	-	72.3	3.76 bd
3'	72.4	3.58 bm	-	-	72.4	3.58 m
4'	73.6	3.36 dd,9.4,9.4	-	-	73.6	3.35 dd,9.3,9.3
5'	69.6	3.60 m	-	-	69.5	3.50 m
6'	18.1	1.17 d,6.2	-	-	18.1	1.12 d,6.1

SB-253514 (1): C17-C22 at 30.03, 30.29, 30.31 (two coincident) and 30.36 (two coincident) ppm. H2' and H3' sharpen to dd,1.6,3.4 Hz and dd,3.5,9.3 Hz after D<sub>2</sub>O exchange. [2'-, 3'- and 4'-OH at 3.81, 3.78 and 3.70 ppm.]

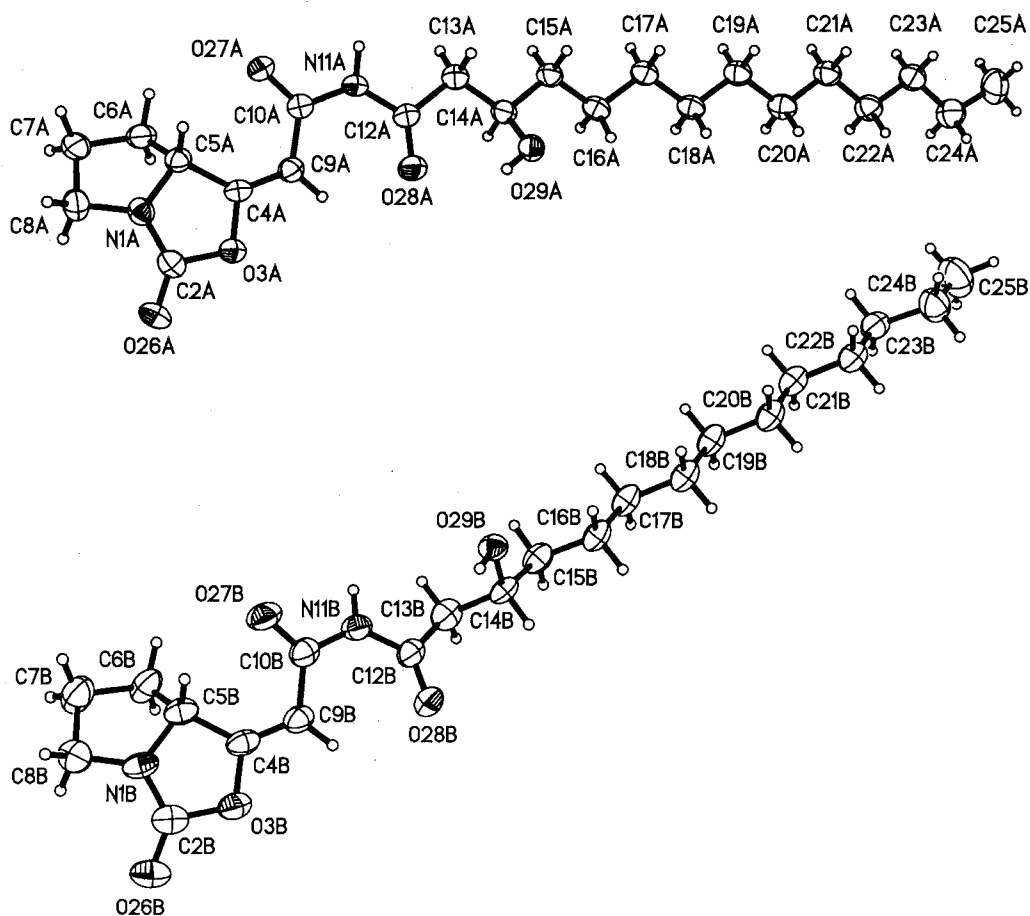
SB-311009 (2): C17-C22 at 30.04, 30.29, 30.32 (two coincident), 30.34 and 30.36 ppm. 14-OH at 3.96 ppm.

could be determined reliably from the diffraction experiment and the *R* configuration was observed for both stereocentres in each of the independent molecules.

The largest conformational difference between molecules A and B is the torsion angle N11-C12-C13-C14, being

-167.5(2)° and 111.7(3)° for the two molecules respectively. Molecules C and D are conformationally identical to A and B respectively, and are related by pseudosymmetry. The tails of neighbouring molecules are in close proximity to one another and extend in the same

Fig. 3. A view of molecules A (top) and B (bottom) of SB-311009 from the crystal structure showing the numbering scheme employed.



Anisotropic displacement ellipsoids for the non-hydrogen atoms are shown at the 50% probability level. Hydrogen atoms are displayed with an arbitrarily small radius.

direction whilst the polar heads cluster together supported by a hydrogen bonding network. Overall this leads to a layered arrangement of heads and tails perpendicular to the crystallographic *b*-axis.

#### Structure of SB-315021

A second family of metabolites with Lp-PLA<sub>2</sub> activity were also identified from DSM11579. These metabolites possessed a different UV profile to the 5,5-series of metabolites but appeared to give an identical series of molecular ions, suggesting they were isomeric to the 5,5-series.

The predominant member of this family of metabolites, SB-315021, was shown by mass spectrometry to be isomeric with SB-253514 (Table 1). The NMR data,

through comparison with that of SB-253514, indicated that SB-315021 possessed the same alkyl chain [ $\Delta\delta_{\text{H}} < 0.03$  ppm and  $\Delta\delta_{\text{C}} < 0.2$  ppm for H14-H25 and C13-C25] and sugar [ $\Delta\delta_{\text{H}} < 0.1$  ppm and  $\Delta\delta_{\text{C}} < 0.3$  ppm] sub-structure as SB-253514 but a different bicyclic moiety. More detailed analysis of the NMR data (COSY and HMBC connectivities as well as <sup>1</sup>H and <sup>13</sup>C NMR chemical shifts) from the bicyclic moiety revealed that the pyrrolidine ring was still present (Table 2). Therefore the structural difference between the two isomeric species was concluded to be in the nature of the second ring of the bicyclic moiety. The observed difference in UV profile (280 nm compared with 252 nm for SB-253514) would appear to support this conclusion since the chromophore is located within this sub-structure of the molecule. Furthermore, the definitive carbonyl stretch of the 5-ring carbamate was no longer

present in the infrared spectrum even though the NMR suggested a carbamate carbon (149.6 ppm) is still present. From the spectroscopic data it was therefore concluded that SB-315021 possessed structure (3) with a 5,7-bicyclic moiety. Whilst the 5,5-bicyclic system is novel, the 5,7-bicyclic system has been found for other metabolites, specifically the cyclocarbamides A and B isolated from *Streptovercillium* sp.<sup>4</sup>). The spectroscopic data for SB-315021 is in good agreement with that reported for the cyclocarbamides.

## Experimental

### General

All NMR experiments were performed on acetone-*d*<sub>6</sub> solutions at 300 K using a Bruker AVANCE 400 spectrometer. Proton NMR chemical shifts were referenced relative to the residual solvent at 2.05 ppm with carbon-13 NMR chemical shifts referenced relative to the solvent signal at 29.8 ppm. Deuterium isotope effects were measured as  $\delta_C$  (NH)- $\delta_C$  (ND) following titration of D<sub>2</sub>O into the NMR solution. FAB mass spectrometry was performed on either a JEOL AX-505HA or Micromass 70-VSEQ using glycerol and PEG400 as matrices. Electrospray mass spectrometry was performed on a Micromass LCT using reserpine as the internal reference. Infrared spectra were acquired at 2 cm<sup>-1</sup> resolution using a Perkin-Elmer 1720X FT-IR spectrometer. (Samples were prepared as KBr discs, except for SB-315021 which was prepared by evaporating a CH<sub>2</sub>Cl<sub>2</sub> solution onto a KBr plate). Raman spectroscopy was performed on a Perkin-Elmer 2000R spectrometer (4 cm<sup>-1</sup> resolution), with the sample contained in a glass capillary. Excitation was from the 1064 nm output of a Nd:YAG laser operating at 1500 mW. Ultraviolet spectroscopy (MeOH/EtOH) was performed on a Perkin-Elmer Lambda 19 UV/Visible spectrophotometer.

### X-Ray Crystallography

Crystals of SB-311009 were prepared by the slow evaporation of a methanol solution at 7°C. A colourless block of dimensions 0.20×0.14×0.14 mm was mounted on a glass fibre using paratone oil and flash frozen to 150 K. Crystal data: C<sub>22</sub>H<sub>36</sub>N<sub>2</sub>O<sub>5</sub>, M=408.53, monoclinic, space group P2<sub>1</sub> (#4), a=7.2617(3), b=78.711(3), c=7.9268(4) Å,  $\beta$ =90.172(4)°, V=4530.8(3) Å<sup>3</sup>, Z=8, D<sub>calc</sub>=1.198 M gm<sup>-3</sup>, F(000)=1776,  $\mu$ (Cu-K $\alpha$ )=0.683 mm<sup>-1</sup>. All measurements were made using a Bruker AXS SMART 6000 diffractometer with graphite monochromated

Cu-K $\alpha$  radiation from a normal focus sealed tube. The diffractometer was controlled using the SMART program<sup>5</sup>). The crystal-detector distance was 11.8 cm. In total 23094 frames were collected with the detector set in four different positions in  $2\theta$ . The exposure time was varied with  $2\theta$  between 4 and 30 seconds, with each frame covering 0.15° in  $\omega$ . Frame integration and data reduction was carried out using the SAINT+ suite of programs<sup>6</sup>). Of the 25718 reflections collected, 11647 were independent ( $R_{int}$ =0.0461) and this represents 92.4% of the unique data to the  $2\theta_{max}$  of 124.14° ( $d$ =0.873 Å). Data were corrected for Lorentz and polarization effects and a Gaussian absorption correction was applied using the measured crystal faces (transmission=0.8787-0.9197). The program SADABS (within SAINT+) was used after this to correct for X-ray absorption of the incident beam caused by the glass mounting fibre. The structure was solved by direct methods and refined by full-matrix least-squares on F<sup>2</sup> using the SHELXTL suite of programs<sup>7</sup>). Atomic coordinates and anisotropic atomic displacement parameters were refined for the non-hydrogen atoms. Hydrogen atoms were included in calculated positions and refined using the riding mode with the exception of the hydrogen atoms attached to heteroatoms, where refinement of the coordinates was allowed with distance restraints. Isotropic atomic displacement parameters for the hydrogen atoms were used as multiples of U<sub>eq</sub> for the attached atom. The final R1 (10436 reflections with  $F_o > 4\sigma(F_o)$ ) and wR2 (all data) were 0.0449 and 0.1173 respectively, with the goodness of fit being 1.025. A final difference Fourier synthesis showed residual electron density between -0.18 and 0.20 eÅ<sup>-3</sup>. The absolute configuration was assigned on the basis of the absolute structure parameter<sup>8</sup>) which refined to 0.00(15). The possibility of missed symmetry was thoroughly investigated. Structure solution and refinement was possible in the orthorhombic space group P2<sub>1</sub>2<sub>1</sub>2<sub>1</sub> (#19) with two independent molecules corresponding to molecules A and B. The monoclinic refinement was superior in every respect and the difference was judged statistically significant<sup>9</sup>). Confidence in the monoclinic model was reinforced by the consistent and reproducible values of  $\beta$  obtained.

### Acknowledgement

The authors would like to thank Dr's ANDY ORGAN and NEVILLE HASKINS for mass spectrometry, IAN LYNCH for UV spectroscopy and Dr's IVAN PINTO and DEIDRIE HICKEY for scientific contributions.

## References

- 1) THIRKETTLE, J.; E. ALVAREZ, H. BOYD, M. BROWN, E. DIEZ, J. HUESO, S. ELSON, M. FULSTON, C. GERSHATER, M. L. MORATA, P. PEREZ, S. READY, J. M. SANCHEZ-PUELLES, R. SHERIDAN, A. STEFANSKA & S. WARR: SB-253514 and analogues; novel inhibitors of lipoprotein associated phospholipase A<sub>2</sub> produced by *Pseudomonas fluorescens* DSM 11579. I. Fermentation of producing strain, isolation and biological activity. *J. Antibiotics* 53: 664~669, 2000
- 2) THIRKETTLE, J.: SB-253514 and analogues; novel inhibitors of lipoprotein associated phospholipase A<sub>2</sub> produced by *Pseudomonas fluorescens* DSM 11579. III. Biotransformation using naringinase. *J. Antibiotics* 53: 733~735, 2000
- 3) KASAI, R.; M. OKIHARA, J. ASAKAWA, K. MIZUTANI & O. TANAKA: <sup>13</sup>C NMR study of  $\alpha$ - and  $\beta$ -anomeric pairs of D-mannopyranosides and L-rhamnopyranosides. *Tetrahedron* 35: 1427~1432, 1979
- 4) ISOGAI, A.; S. SAKUDA & K. SHINDO: Structures of cyclocarbamides A and B, new plant growth regulators from *Streptoverticillium* sp. *Tetrahedron Lett.* 27: 1161~1164, 1986
- 5) Bruker: SMART. Version 5.057c (NT). Area detector control software. Bruker AXS Inc., Madison, Wisconsin, USA, 1999
- 6) Bruker: SAINT+. Version 5.02 (NT). Area detector integration and data reduction software. Bruker AXS Inc., Madison, Wisconsin, USA, 1998
- 7) Bruker: SHELXTL. Version 5.10 (IRIX). Structure determination programs. Bruker AXS Inc., Madison, Wisconsin, USA, 1997
- 8) FLACK, H. D.: On enantiomorph-polarity estimation. *Acta Cryst.* A39: 876~881, 1983
- 9) HAMILTON, W. C.: Significance tests on the crystallographic *R* factor. *Acta Cryst.* 18: 502~510, 1965